Impact of middle range energy electron precipitations on polar winter ozone losses

Kseniia Golubenko[1], *Irina* Mironova[1], and *Eugene* Rozanov[2,3]

[1]Institute of Physics, Saint Petersburg State University, Saint Petersburg, Russia
[2]Physikalisch-Meteorologisches Observatorium, World Radiation Center, Davos, Switzerland
[3]Institute for Atmospheric and Climate Science, ETH Zurich, Zurich, Switzerland

Abstract. In this paper we present the study of polar winter atmospheric response to middle range energy electron precipitations. We analse the variability of the odd nitrogen group NOx, hydrogen group HOx in the polar wonter atmosphere and estimate the ozone (O3) depletion caused by the middle range energy electron precipitations. For the study we exploit 1-D radiative-convective model with interactive neutral and ion chemistry. Ionization rates induced by middle-energy electrons were taken from the CMIP6 (Coupled Model Intercomparison Project Phase 6) solar forcing dataset. The atmospheric response to ionization rates induced by middle-energy electrons during polar night consists of increase of mesospheric HOx by 0.1-0.4 ppbv and NOx by 10-90 ppbv driving ozone losses up to 5% over zonal band of about 75^0 NH.

Introduction

Energetic electrons are accelerated in the terrestrial magnetosphere and magnetotail during auroral substorms and geomagnetic storms and then precipitate into the atmosphere at high latitudes [e.g., 1]. Primary collision processes with the most abundant species N2, O2, and O lead to the formation of nitric oxides primarily in the mesosphere and lower thermosphere (65—150 km) and initiate . ion and neutral chemistry reactions affecting many other trace gases [2]. Nitric oxides can be transported down into the stratosphere below 45 km altitude in large-scale downward motions over polar latitudes during winter, and destroy ozone there in catalytic cycles [3, 4]. Ozone plays major role in radiative heating and cooling of the middle atmosphere. Therefore, ozone changes directly affect stratospheric temperatures and start a chain of dynamical coupling mechanisms alternating atmospheric temperatures and circulation over large areas down to the troposphere [5,6,7].

The impact of ionization rates induced by energetic particles of different origin on parameters of polar atmosphere, chemical composition of the atmosphere and dynamics was extensively evaluated during last decades [e.g., 8-15].

In the framework of CMIP6 (Coupled Model Intercomparison Project Phase 6) several scenarios of the forcing from energetic particle precipitations were developed [16]. The ionization rates caused by MEEP (middle range energy electrons precipitation from 30 keV

* Corresponding author: golubksen@yandex.ru

to 1 MeV) were parameterized as a function of geomagnetic activity indices using the POES satellite data [17].

In this paper we show the importance of MEE for chemical composition of the polar winter atmosphere using the results of 1-D radiative-convective model with interactive neutral and ion chemistry considering ionization rates induced by MEEP.

Materials And Method

The investigation is performed with the 1-D radiative-convective model with interactive neutral and ion chemistry (RCMC).The RCMC was developed at PMOD/WRC [18, 19]. The model consists of the radiation, chemistry, convective adjustment, and vertical diffusion modules. The atmosphere is divided into 40 layers that extend from the ground to 100 km. The input solar spectrum covers the wavelength range from 121 to 750 nm and is divided into 73 intervals. The model computes the temperature profile and the distribution of 43 neutral chemical species of the oxygen, nitrogen, hydrogen, carbon, chlorine, and bromine groups and 48 ions (31 positive and 17 negative). The chemical module also treats ion chemistry as described in [20]. The chemical solver utilizes the implicit iterative Newton-Raphson scheme [21]. The vertical turbulent transport of long-lived species was calculated using typical annual mean values of the vertical eddy diffusion coefficients.
The atmospheric ionization rates induced by MEEP (an input parameter in RCMC) are taken from CMIP6 solar forcing dataset [16].
All runs are executed for 28 winter day with MEEP during february of 2013. All experiments are started from the same initial atmospheric conditions for polar winter night. The reason for choosing winter season for investigation of MEEP atmospheric effects is based on previous obtained results that show stronger effects [e.g., 22, 23].

Results

The ionization rates during February of 2013 are shown in Figure 1. The enhanced ionization from the energetic particles precipitation locates in the mesosphere and lower thermosphere, with the highest ionization ratesbetween 67 km and 87 km for strong MEEP (middle-energy electron precipitation).

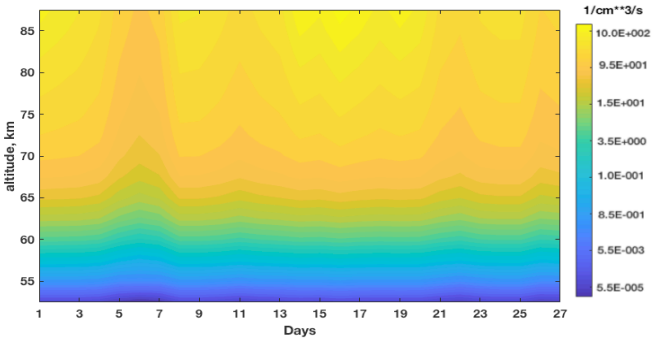

Fig. 1. Ionization rates induced by MEEP during Febuary of 2013.

Figures 2- 4 show results simulated by RCMC driven by MEEP forcing. Figure 2 shows NOx production after MEEP, when responses are most pronounced. The top panel demonstrates the NOx concentration response. As can be seen, increasing ionizations rates (IR) leads to more intensive NOx production. During 5, 8 February and 21, 24 February, when IR were increased by up to 10 times (see Fig.1) , NOx production at the next day after MEEP is maximized. The increase of NOx mixing ratio due to MEEP usually varies between 10 and 100 ppbv. These values are smaller than after solar proton events (SPE), when the magnitude of NOx increase can reach 100-1000 ppbv [8].

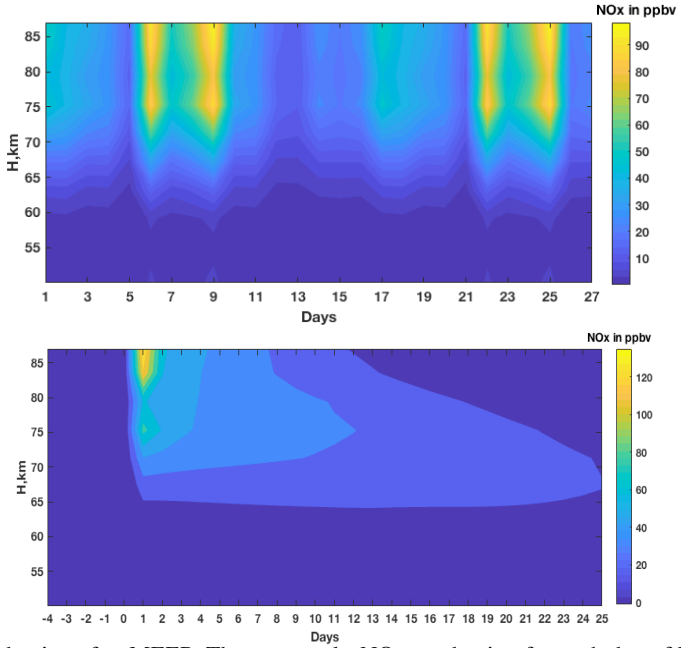

Fig. 2. NOx production after MEEP. The top panel - NOx production for each day of February 2013. The bottom panel – results of superposed epoch analysis where the key day – days of MEEP.

The bottom panel of Figure 2 show results of superposed epoch analysis where as key day were taken 28 days of MEEP. Here one can see strong NOx increase in altitudinal range about 65 km -87 km. MEEP diffusion transfer, or MEEP direct effect driving to NOx production can be important into polar night atmosphere up to one month.

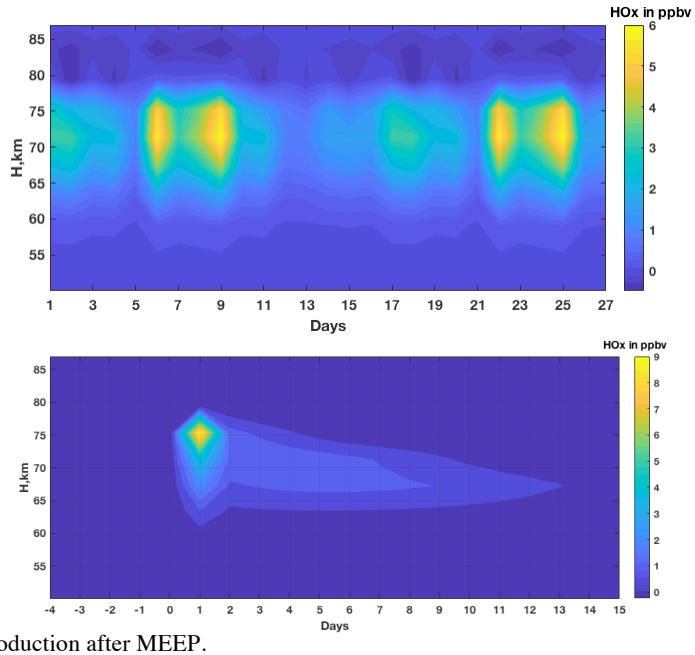

Fig. 3. HOx production after MEEP.
The top panel - HOx production for each day of February 2013. The bottom panel – results of superposed epoch analysis where the key days – days of MEEP.

Figure 3 illustrates HOx production caused by MEEP. The top panel increasing ionizations rates (IR) provide NOx production more intensive. At Fig.1 one can see that IR increasing in order, duirng 5, 8 February and 21, 24 February, lead to maximum of HOx production at the next day after MEEP. HOx production due to MEEP is confined to 57 km -77 km region. Unlike NOx, HOx increase varies between 2 and 6 ppbv, see Figure 3. For winter season it is typical situation due to atmospheric conditions without UV-radiation. But these low values are large enough to increase ozone losses by about 5 % in the upper mesosphere. Like as NOx, HOx production by MEEP induced ionization rates.
The bottom panel of Figure 3 show results of superposed epoch analysis where as key days were taken 28 days of MEEP. It shows that HOx content increase is the most pronounced in the altitudinal range about 62 km -80 km.

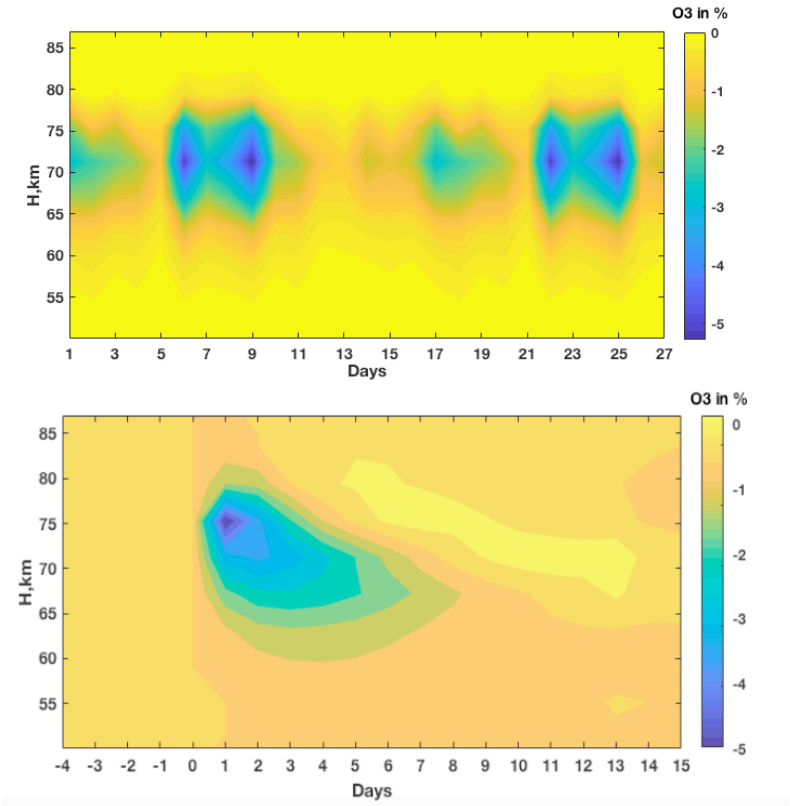

Fig. 4. Ozone losses after MEEP. The top panel – O3 losses are driving by MEEP during each day of February 2013. The bottom panel – results of superposed epoch analysis where the key days – days of MEEP.

Figure 4 shows ozone losses after MEEP in 57 km - 77 km layer. In Figure 4 ozone losses reach up to -5% under MEEP influence. A peaks of ozone losses correspond to days of maximal NOx and HOx production. Maximum altitude for ozone loss is about 70 km - 75 km.

Conclusion

The response of polar winter atmosphere to middle-energy electron precipitation is investigated using 1-D radiative-convective model with interactive neutral and ion

chemistry. The simulated results show increase of mesospheric HOx by 0.1-0.4 ppbv and NOx by 10-90 ppbv driving ozone losses up to 5% over zonal band of about 75° NH.

Acknowledgments

This work was done in the frame the ISSI & the ISSI- BJ project "Relativistic electron precipitation and its atmospheric effect". ER participated in the data analysis and his work was supported by the Russian Science Foundation (grant no. 17-17-01060).

References

1. R. Barra, D. Llanwyn Jonesb, C.J. Rodgerc, Journal of Atmospheric and Solar-Terrestrial Physics 62 (2000) 1689–1718, (2000).
2. Rusch, D. W., J.−C. Gerard, S. Solomon, P. J. Crutzen, and G. C. Reid, Planet. Space Sci., 29, 767–774, (1981).
3. Solomon S., D.W. Rusch, J.C. Gerard, Planet. Space Sci., 29, 885-894, (1981).
4. Porter, H. S., C. H. Jackman, and A. E. S. Green, J. Chem. Phys., 65, 154-167, (1976)
5. Seppälä, A., M. A. Clilverd, M. Beharrell, C. J. Rodger, P. T. Verronen, M. E. Andersson, and D. A. Newnham, Geophys. Res. Lett., 42, 8172–8176, (2015).
6. Rozanov, E., Calisto, M., Egorova, T., Peter, T., & Schmutz, W. Surveys in Geophysics, 33, 483–501, (2012).
7. Mironova, I. A., Aplin, K. L., Arnold, F., Bazilevskaya, G. A., Harrison, R. G., Krivolutsky, A. A., et al. Space Science Reviews, 194, 1–96, (2015).
8. Jackman, C. H., Marsh, D. R., Vitt, F. M., Garcia, R. R., Fleming, E. L., Labow, G. J., Randall, C. E., López-Puertas, M., Funke, B., von Clarmann, T., and Stiller, G. P., Atmos. Chem. Phys., (2008).
9. P.Arsenovic, E.Rozanov, A.Stenke, B.Funke, Journal of Atmospheric and Solar-Terrestrial Physics. Volume 149, November 2016, 180-190, (2003).
10. Calisto, M., Usoskin, I., Rozanov, E., and Peter, T., Atmos. Chem. Phys., 11, 4547–4556, (2011).
11. Mironova, I.A., Artamonov, A.A., Bazilevskaya, G.A., Rozanov, E.V., Kovaltsov, G.A., Makhmutov, V.S., Mishev, A.L., Karagodin, A.V., Geophys. Res. Lett. 46, 990–996., (2019).
12. Mironova, I.A., Desorgher, L., Usoskin, I.G., Flückiger, E.O., Bütikofer, R., Geophys. Res. Lett. 35, L18610, (2008).
13. Mironova, I.A., Usoskin, I.G., Atmos. Chem. Phys. 13, 8543–8550. https://doi.org/10.5194/\ignorespacesacp- 13- 8543- 2013, 2013.
14. Mironova, I.A., Usoskin, I.G., Environ. Res. Lett. 9, (2014).
15. Mironova, I.A., Usoskin, I.G., Kovaltsov, I.G., Petelina, S.V., Atmos. Chem. Phys. 12, 769–778, (2012).
16. Matthes, K., Funke, B., Andersson, M. E., Barnard, L., Beer, J., Charbonneau, P., et al. Geos Model Development, 10, 2247–2302, (2017).
17. van de Kamp, M., A. Seppälä, M. A. Clilverd, C. J. Rodger, P. T. Verronen, and I. C. Whittake, J. Geophys. Res. Atmos., 121, (2016).
18. Egorova, T., I. Karol, and E. Rozanov, Phys. Atmos. Ocean (Russ. Acad. Sci.), 33, 492–499, (1997).

19. Rozanov, E., T. Egorova, C. Fröhlich, M. Haberreiter, T. Peter, and W. Schmutz, ESA SP-508, pp. 181–184, (2002).
20. Ozolin, Y., I. Karol, E. Rozanov, and T. Egorova, Izv., Atmos. Ocean. Phys., 5(6), 737–750, (2009).
21. Rozanov, E., V. Zubov, M. Schlesinger, F. Yang, and N. Andronova, J. Geophys. Res., 104, 11755–11782, (1999).
22. Sinnhuber, M., H. Nieder, and N. Wieters, Surv. Geophys., Springer, Dordrecht, Netherlands, (2012).
23. Seppälä, A., M. A. Clilverd, M. Beharrell, C. J. Rodger, P. T. Verronen, M. E. Andersson, and D. A. Newnham, Geophys. Res. Lett., 42, 8172–8176, (2015).